2022

Two mechanisms for formation of ferronematic phase studied by dielectric spectroscopy

Neelam Yadav
Trinity College Dublin, Ireland

Yuri Panarin
Technological University Dublin, yuri.panarin@tudublin.ie

J.K. Vij
Trinity College Dublin, Ireland, jvij@tcd.ie

See next page for additional authors

Funder: Irish Research Council

Two mechanisms for formation of ferronematic phase studied by dielectric spectroscopy

Neelam Yadav[1], Yuri P. Panarin[1,2], Jagdish K. Vij[1*], Wanhe Jiang[3], Georg H. Mehl[3]

[1]Department of Electronic and Electrical Engineering, Trinity College Dublin, The University of Dublin, Dublin 2, Ireland
[2]Department of Electrical and Electronic Engineering, TU Dublin, Dublin 7, Ireland
[3]Department of Chemistry, University of Hull, Hull HU6 7RX, UK

Abstract

A non-chiral ferroelectric nematic compound DIO was studied by dielectric spectroscopy in the frequency range 0.01 Hz to 10 MHz over a wide range of temperatures. The compound exhibits three nematic phases on cooling from the isotropic phase, viz. the ordinary paraelectric nematic N; intermediate nematic N_X and ferroelectric N_F phases. The lower frequency relaxation process P_1 is similar to those observed in other ferronematic compounds. It is a continuation of the molecular flip-flop mode in the isotropic phase and corresponds to the collective movement of dipoles which are strongly coupled with splay fluctuations in the nematic phases. In addition to this process, the studied compound DIO shows another collective relaxation process in both paraelectric nematic phases. The high-frequency P_2 originates from the polar/chiral domains which appear due to spontaneous symmetry breaking in achiral system. Both the collective processes, P1 and P2, show soft mode-like behavior on cooling to the N_X-N_F phase transition and therefore independently contribute to the formation of ferronematic phase.

*jvij@tcd.ie

I. INTRODUCTION

Since the discovery of the liquid crystalline state made first in the studies of the derivatives of cholesterol, the chirality and polarization properties of liquid crystals are entirely related to the molecular chirality. In this case, at least one of the carbon atoms in the molecule is connected to four different substituents. During the last couple of decades such features were also observed in achiral LC systems composed of bent-core molecules [1] and the bent bi-mesogens that exhibit the twist-bent LC state [2]. In such systems, achiral molecules may form the so-called "chiral phases", which exhibit optical activity and/or spontaneous polarization. Finally, a new, long-awaited Ferroelectric Nematic phase [predicted more than a century ago by P. Debye [3] and M. Born [4], was discovered in 2017 independently by two research groups [5,6]. In one of the first publications for the ferroelectric nematic, extremely large dielectric permittivity ~10^4 and high spontaneous polarization of ~ 4.4 μC cm^{-2} were reported in the compound DIO [5]. This material exhibits three variants of nematic phases, such as the ordinary paraelectric nematic (N), an intermediate unknown nematic (N_X), and ferroelectric nematic (N_F), which were originally named as M1, M2 and MP correspondingly. The compound DIO was recently reexamined by the Boulder group [7] and they found from XRD that the intermediate N_X (or M2) existing between the paraelectric N and the ferroelectric N_F is density modulated phase, with a period of 8.6 nm with antiparallel and slightly splayed director distribution and suggested it to be antiferroelectric SmZ_A. While Sebastian et al. prefer to call it N_S [8] since it belongs to the class of modulated nematic phases where periodicity of modulation is dependent on the property of the material.

The other ferroelectric nematic compound RM734 and its homologues synthesized by Mandle et al [6] possesses a large molecular dipole moment and exhibit two distinct nematic mesophases, ordinary paraelectric N and N_X, with antiparallel molecular associations separated by a weak first-order transition [9]. Later, Mertelj et al [10] showed that N_X subphase forms a splay modulated structure with period of 5–10 microns presumably due to the wedge molecular shape of the RM734 molecules and they introduce it as splay nematic phase (N_S) [11,12,13]. The N-N_S phase transition bears resemblance to the ferroelectric to ferro-elastic transition that occurs via flexoelectric coupling [11]. Chen *et al.* [14] gave the first major demonstration of ferroelectricity in N_X phase and confirmed that it is ferroelectric nematic (N_F) phase.

These newly discovered phases display fascinating properties currently being studied by several research groups with the main objective of obtaining better understanding of the origin of ferroelectricity in achiral nematics [15]. Novel nematic-nematic phase transitions were

recently reported. Manabe *et al.* [16] synthesized a compound that shows a direct transition from the isotropic state to the N_F phase while Saha *et al*. reported an LC material that exhibits multiple ferroelectric nematic phases [17]. In this paper, we investigate the dielectric properties of the compound DIO [5] using dielectric spectroscopy, focusing on the study of high temperature subphases, N and N_X (SmZ_A or N_S) and make a detailed analysis of the relaxation processes observed in the system. Dielectric spectroscopy is a powerful method for studying dipolar response of a system subject to a weak electric field and for exploring the dielectric relaxation phenomena in dielectric materials. While the technique does not yield direct information of the micro/nano structure of the material, nevertheless some of the structural details are deduced indirectly from the dielectric spectra. The results from DS complement those obtained using other methods: X-ray diffraction, SHG etc. It is an excellent probe for studying the molecular dynamics of the dipolar molecules and in some ways, it is superior to the electro-optical methods since the prevailing structure of the LC medium is not significantly perturbed by the weak external field. Rearrangement of the molecular orientational ordering and of the rotational distribution of dipoles induced by a weak probe field govern the temperature dependent dielectric response of the LC phase under investigation. Dielectric spectroscopy has been used to investigating dielectric properties of ferroelectric nematics [13,18,19]. In the past, this technique has successfully been used to study different phases of LCs: ferroelectric SmC [20], TGBA [21], ferrielectric [22,23] and antiferroelectric SmC-like LCs [24], de Vries phase [25], bent-core nematics [26,27] and SmCP [28].

The molecular structure and the phase transition temperatures recorded at a scanning rate of 0.2 ^oC/min. for DIO are given in Fig.1.

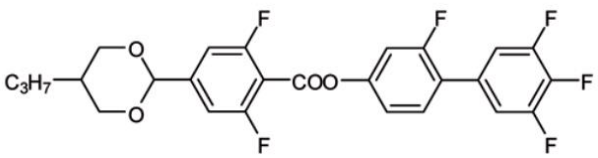

On cooling: X - MP (N_F) 66.8 M2 (SmA_Z or N_X) 83.5 M1 (N) 173.8 Iso (˚C)

FIG. 1. Molecular structure, the phase-sequence and the transition temperatures of the synthesized DIO compound. The nomenclature of the phases here is drawn from the papers of Nishikawa *et al*. [5] and of Chen *et al*. [7].

This compound was resynthesized by the group of G. H. Mehl (Hull, UK) and shows phase transition temperatures lower than originally reported [5]. In general, the transition

temperature depends on the intermediates used in the synthesis and the rate of scanning the sample cell.

II. EXPERIMENTAL DETAILS

The complex dielectric permittivity measurements are made using broadband Alpha high-resolution dielectric analyzer (Novocontrol GmbH, Germany). We use commercial cells (EHC ltd, Japan) with low-resistance ITO electrodes (10 Ω/cm^2) coated with the polyimide (LX-1400, Hitachi-Kasei) alignment layers of ~ 20 nm thickness for planar alignment, while cetyl-trimethyl-ammonium-bromide used to obtain homeotropic alignment. A polyester roll with fiber length and roll diameter of 8 mm and 58 mm respectively was used for rubbing. The rubbing is performed with a rotational speed of 600 rpm and the stage speed is kept at 30 mm/sec. The sample cell was filled at a lower temperature (150 ^{o}C) by capillary action and then heated to its isotropic state. Measurements of the dielectric permittivity are made on aligned thin cells of liquid crystalline samples under cooling. Temperature of the cell is varied in steps of 1 °C and measurements made under the application of a weak external voltage of 0.1 V. Results of the experiment are repeatable, furthermore no decomposition of the material is observed as confirmed by Thermo-Gravimetric Analyzer (TGA). The temperature of the cells with the sample aligned was stabilized to within ±0.02 °C.

III. RESULTS AND DISCUSSION

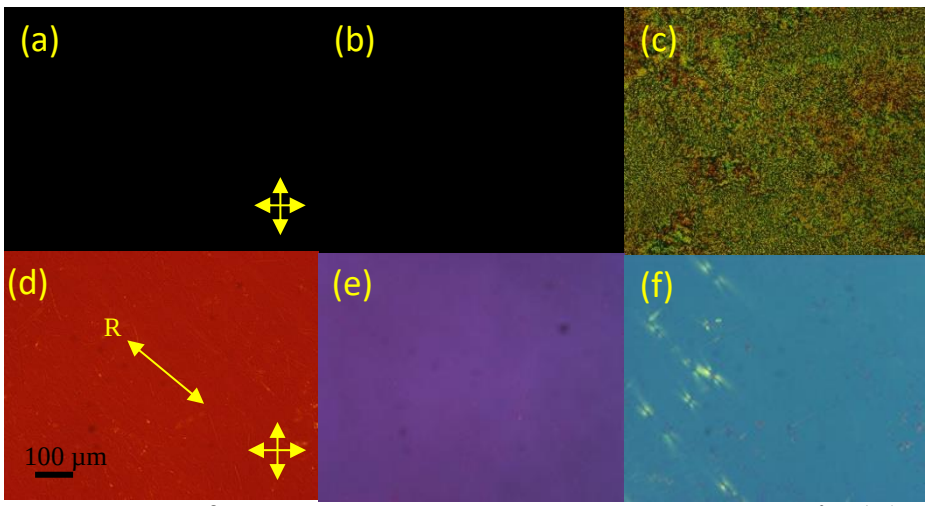

FIG. 2 Textures of DIO recorded in homeotropic cells at (a) 130 ˚C (N), (b) 70 ˚C (N_X) (c) 60 ˚C (N_F) and in planar aligned cells of 4 µm thickness (R is the rubbing direction) at (d) 130 ˚C (N) (e) 70 ˚C (N_X) (f) 60 ˚C (N_F).

Before making dielectric measurements, textures of the cells were recorded by using Polarized Optical Microscopy (POM). This was done to verify the alignment of the molecules in both homeotropic and planar configurations. Fig. 2a-2b shows that the molecules are perfectly

aligned homeotropically in the N and N_x phases. But in the N_F phase (Fig 2c), sandy or grainy texture with no clear extinction is visible. The textures of planar-aligned cells (Fig 2d-f) display perfect homogeneous alignment in all the three phases.

Temperature dependencies of the real and the imaginary parts of the complex permittivity in the frequency range of 0.1 Hz to 10 MHz were recorded for both homeotropic and planarly aligned cells. The observed temperature dependent dielectric loss spectra of the longitudinal

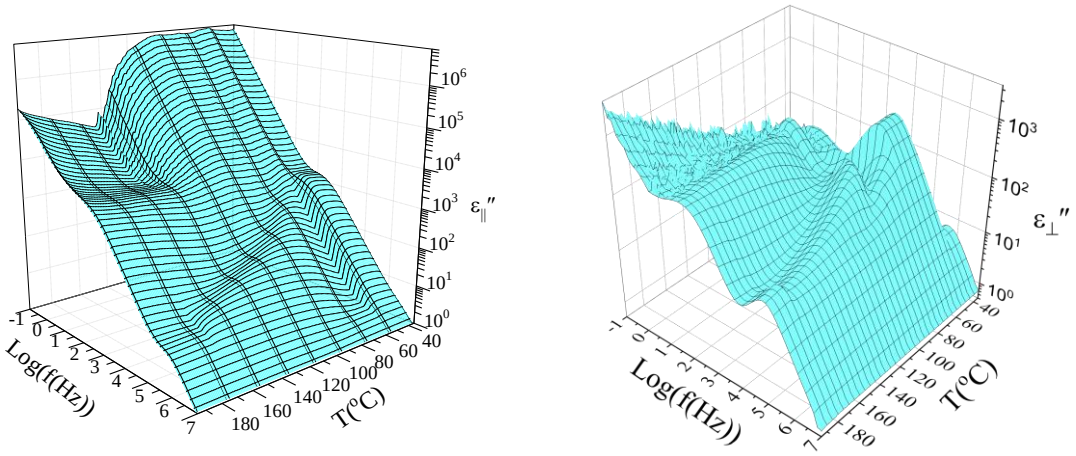

(a) (b)

FIG. 3. Three-dimensional (3D) dielectric loss spectra of DIO in a cell of thickness 4 μm (a) homeotropic and (b) planar homogeneously aligned cells.

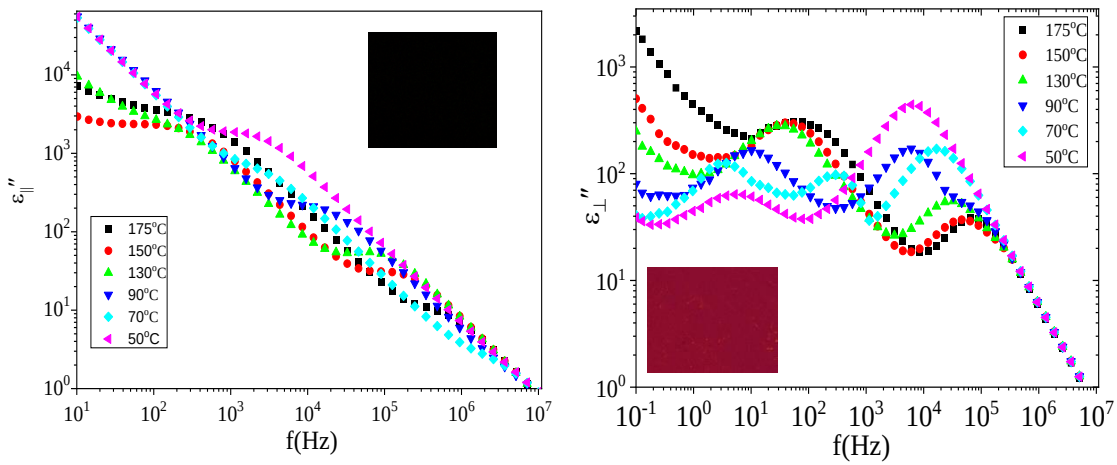

(a) (b)

FIG. 4. Two dimensional cuts of the 3D plots of the dielectric loss spectra versus frequency (Fig. 3) in different phases: I at 175 ºC; at 150 ˚C, 130 ˚C, 90 ˚C all in M1 (N); at 70 ˚C in M2 (N_X); and at 50 ˚C in MP (N_F**)** phase (a) homeotropic cell and (b) planar aligned cell. The Insets in figures depict texture of the aligned DIO sample: homeotropic (a) and in a planar aligned cell (b) both in the nematic phase.

($\varepsilon_{\parallel}''$) and the transverse ($\varepsilon_{\perp}''$)) components of the complex permittivity are shown in Fig. 3 for a cell of 4 μm. Fig. 4 presents the dielectric loss spectra at different temperatures in all the four phases: 175 °C (I), at 150 ˚C, 130 ˚C, 90 ˚C in N, at 70 ˚C in N_X; and in the N_F at 50 ˚C. The spectra are analyzed using WINFIT software, developed by Novocontrol GmbH, Germany. The complex permittivity data are fitted to the Havriliak - Negami equation:

$$\varepsilon^* = \varepsilon_\infty + \sum_{j=1}^{n} \frac{\delta\varepsilon_j}{\left[1+(i\omega\tau_j)^{\alpha_j}\right]^{\beta_j}} - \frac{i\sigma}{\varepsilon_0\omega} \qquad (1)$$

where ε^* is the complex dielectric permittivity, ε_∞ is the high frequency dielectric permittivity including electronic and atomic permittivity of the material, ω ($=2\pi f$), is the angular frequency

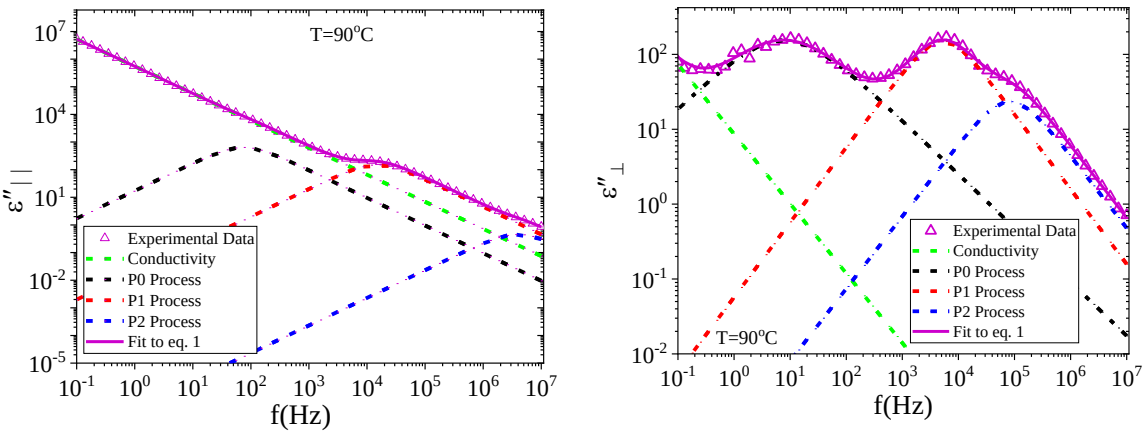

FIG. 5. Frequency dependence of the dielectric loss at a temperature of 90 °C in the nematic phase. The triangular symbols represent the experimental data, solid magenta line is the fit to eq. 1, green dash lines indicate conductivity while the black, red, and blue dash lines denote the three processes viz. P0, P1 and P2 respectively.

of the probe field, ε_o is the permittivity of the free space, σ is the dc conductivity, τ_j is the relaxation time, $\delta\varepsilon_j$ is the dielectric amplitude or strength of the relaxation process, α_j and β_j are the symmetric and asymmetric broadening parameters which reflect distribution of the relaxation times. The parameter with the subscript j corresponds to the j^{th} relaxation process. The experimental data are fitted to the three processes, i. e. n = 3. Figure 5 show the examples of fitting of the imaginary parts of the permittivity with separate relaxation processes observed at 90 °C. The distribution parameters for the relaxation processes P1 and P2 are found as: α_j = 1 and β_j = 1, which reflect the Debye type of relaxation processes. The temperature dependencies of the fitting parameters in terms of the dielectric strength and the relaxation frequencies are shown in Figure. 6 both for the homeotropic and the planar-aligned cells.

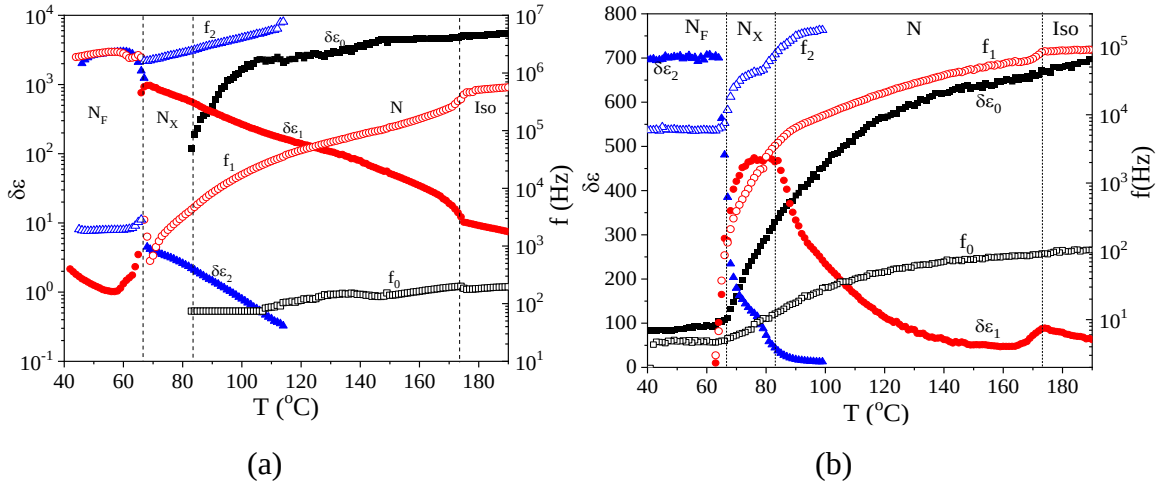

FIG. 6. Temperature dependence of the relaxation processes: (a) homeotropic cell, dielectric strength (δε) (filled data points) and the relaxation frequency (f) (unfilled data points) in a cell of 4 μm cell spacing and (b) planar homogeneously aligned cells. Data points shown in color: Black (P_0), Red (P_1) and Blue (P_2).

A first glance at the Figures 3-6 shows several unusual features. Unlike the ordinary liquid crystalline nematic phase which shows only the molecular relaxation processes which occur at higher frequencies, here up to three collective relaxation processes are observed. These processes are denoted as P_0, P_1, and P_2 with an increase in the relaxation frequency.

P_0 is the AC conductivity low frequency process, which is due to the separation of ions and accumulation of charge on the alignment layers. The dielectric strength of this process in homeotropic cells is much higher than in planar-aligned cell due to the ease in the migration of ions occurring along the molecular director than perpendicular to it. This parasitic, non-molecular pseudo-relaxation process is out of the current interest of this manuscript and hereafter is excluded from further discussions.

Another remarkable feature is extremely high dielectric constant of the order of 1000. There may be some problem in the interpretation of the measured spectra, discussed by the Boulder group [29]. Usually, the test cell consists of ITO conducting electrodes coated with thin polymer layer to obtain planar/homeotropic homogeneous texture. If the testing material possesses small/moderate dielectric constant, the capacitance of the LC layer is much smaller than the capacitance of polymer layers which can be ignored, and analysis of the dielectric spectra is rather straightforward. However, some ferroelectric smectic materials possess high spontaneous polarization. Therefore, the dielectric constant and capacitance of the LC layer becomes compatible to the capacitance of the alignment layers which are connected in series to the LC layer. This effect was noticed and discussed elaborately in other articles [29,30].

Briefly, the total capacitance of the test cell can be represented by two capacitances of: (i) LC layer (C_{LC}) and double alignment layer (C_a) connected the series. The total capacitance in series $C_T = \frac{C_{LC} \cdot C_a}{C_{LC}+C_a}$ and $C_T|_{C_{LC} \gg C_a} = C_a$ and $C_T|_{C_{LC} \ll C_a} = C_{LC}$. Equating $C_{LC} = \frac{\varepsilon_{LC}\varepsilon_o A}{d_{LC}}$ and $C_a = \frac{\varepsilon_a \varepsilon_o A}{d_a}$ we can find the maximal value of the apparent (or measured) dielectric constant as $\varepsilon^*_{LC} = \frac{\varepsilon_a d_{LC}}{d_a}$. Taking d_{LC}=4 μm, d_a=40 nm and $\varepsilon_a \approx 5$ the maximal value of apparent dielectric constant $\varepsilon^*_{LC} \approx 500$, which is in good agreement with the experimental value of 700, Fig. 2b. It means that the experimental value $\varepsilon^*_{LC} \approx 700$ is not a real dielectric constant ε^*_{LC} of studied material and an apparent value limited by the capacitance of double polymer layer as described in [29] and this capacitance cannot be ignored and straightforward analysis of the dielectric spectra is not applicable in this case. Clark et al [29] showed that the minimization of electrostatic energy orients spontaneous polarization screening the external electric field in LC and the voltage applied to the cell appears across the polymer layers. They suggest that this coupling of orientation and charge creates a combined Polarization-external Capacitance Goldstone (PCG) reorientation and developed a comprehensive theoretical analysis of this mode. Thus, the measured dielectric spectra should be understood as apparent values, which are related to the dielectric constant of the liquid crystal in a complex way which was analytically described for different combination of the parameters of material [30]. So far, the structure and properties of ferroelectric subphase N_F have been extensively studied.

However, as mentioned above our major focus is on the study of the high-temperature phases, N and N_X (SmZ_A or N_S) and we make a detailed analysis of the relaxation processes observed in the system. In this temperature range the dielectric constant is relatively low, i. e. $C_T|_{C_{LC} \ll C_a} = C_{LC}$, so the simple analysis is applicable for this case.

In total, two collective relaxation processes are observed in the studied compound DIO whose physical origin and the properties are discussed below.

The origin and properties of process P_1: The temperature dependencies of the dielectric parameters of the mid-frequency relaxation process P_1 are shown in Figs.6a ($\varepsilon_\parallel$) and 6b ($\varepsilon_\perp$). The process P_1 exists in the entire range of temperature. Permittivity in the isotropic phase is given by the formula, $\varepsilon_{Iso} = (\varepsilon_\parallel + 2\varepsilon_\perp)/3$. Hence, on phase transition from the isotropic (Iso) state to the N phase, the dielectric strength of this process should increase to $\varepsilon_\parallel$ in a homeotropic cell and reduce to $\varepsilon_\perp$ in a planar aligned cell, as shown, respectively, in Figs. 6a and 6b. This observation supports the assignment of P_1 i.e., in the isotropic phase to the flip flop rotation of individual molecules around their short axis which agrees with the conclusion made in a recent

publication [11] that the dipole fluctuations are related to the collective rotation of molecules about their short molecular axis. In general, this molecular mode should normally exist in the N phase too. In this case, the temperature dependence of the relaxation frequency of the molecular relaxation process should follow the Arrhenius behavior, $f(T) = Ae^{\frac{-E_a}{RT}}$, i.e., the plot of log frequency f(T) as a function of 1/T should be a straight line, but it is not followed here. Instead, the temperature dependence of the frequency of this mode shows critical, soft mode - like behavior [8], i.e., the relaxation frequency decreases linearly on approaching the phase transition to N_F. On the transition to the nematic phase, the relaxation process involves the dynamics of short-range correlated groups of molecules. On further cooling, the correlation length (and the volume) continues to grow in the N and N_X phases and the relaxation frequency of P_1 decreases with a reduction in temperature as ~ ($T-T_{NX}$). Thus, P_1 exhibits soft mode - like behavior with a critical temperature occurring at the N_X-N_F phase transition; this being a characteristic feature of the second–order phase transition. Surprisingly the dielectric strength does not follow to soft mode behavior in N_X phase, it initially saturates and then decreases on cooling down to N_F. However, this inconsistency has a simple explanation. The maximum dielectric strength is limited by the capacitance of double alignment layer, so that $\delta\varepsilon_1 + \delta\varepsilon_2 <$ 700 and the apparent value of $\delta\varepsilon_1$ drops due to the faster grow of $\delta\varepsilon_2$.

It is important to mention here that the other ferronematic compound RM-734 and its homologous show only one collective relaxation process in the paraelectric nematic phase [11] which is similar in behavior to mode P_1 (Fig.6 red) i.e. (i) it lies in similar frequency range; (ii) it shows soft mode-like temperature behavior on transition to ferronematic phase; (iii) it exists in both isotropic and paraelectric nematic phases; (iv) it is detected with lower frequency than in the I phase. Therefore, we can assign P_1 to the collective mode as observed in RM734 which was attributed to the "amplitude mode" i.e., the collective movement of dipole moments [11] These are strongly coupled with the splay fluctuations and promote the growth of the polarization.

The origin and the properties of process P2: In general, the temperature dependencies of the dielectric parameters of the high–frequency relaxation process P2 are similar to the mid-frequency relaxation process P1. However, P2 does not exist in the isotropic phase but it emerges in the nematic phase at ~110 ˚C. Most likely this mode exists even at higher temperatures, starting from Is-N phase transition but it may be too weak to be visible. This means that in the paraelectric phases there exist some polar domains with limited correlation length which grow on cooling and finally transform to phason ferroelectric mode (or

Goldstone mode) in the N_F phase. This relaxation process shows soft mode like behavior at both phase transitions and can be assigned to the amplitude "ferroelectric mode'' as the process P1 but it obviously must have a different physical mechanism. This mode is not present in RM734 series compound; therefore, DIO must have some additional property/feature which is responsible for P2. This feature can be observed from POM study of this compound which is discussed in detail in Ref. [31]. In this and in previous studies the textures of planar cell with antiparallel rubbed surfaces are homogeneous. However, in cells made with only one rubbed surface and the other being non-rubbed showed presence of optically active domains of opposite chirality just below Is-N phase transition. In such conditions, where position of director on rubbed surface is fixed along the rubbing direction while it is degenerate on the other (untreated) surface, i.e. the structure follows to the natural activity of the sample. This means that the achiral DIO molecules are segregated into two types of optically active domains. Such segregation of achiral molecules was observed in isotropic phase as well [32]. Spontaneous polarization and polarity are usually related to the optical activity as in the case of Ferroelectric LCs. Also, recent study [33] shows that DIO doped with optically active dopants (OAD) give rise to new discovery of polar cholesteric phase, N_P^*. In this system, a collective mode is observed in the paraelectric cholesteric, which demonstrates a soft mode behavior on approaching the lower temperature N_P^* phase, similar to that observed by us in the pure achiral DIO. In the former case, the chiral dopant is an explicit prerequisite for ferroelectricity whereas in the latter case, this arises implicitly due to chiral segregation of domains of the opposite optical activity. On the other hand, the optical textures of RM734 series in the same cell geometry shows perfect homogenous alignment with no sign of optical activity. So, such spontaneous symmetry breaking, is exclusively the property of DIO and is not reported in ferronematic compounds. This explains the origin of the additional relaxation process, P2 mode. At the phase transition, the achiral molecules begin segregation to form chiral domains of helical molecular conformers of opposite sense. This is because the molecules of the same helical sense are more densely packed than the opposite. Such chiral and polar domains are more favorable than racemic due to the lower excluded volume. The correlation length of these domains grows on cooling, and finally occupies the entire volume at transition to the ferroelectric nematic phase. Therefore, in addition to the amplitude mode, (process P1 in our case), we have another collective process due to the chiral segregation.

IV. CONCLUSIONS

In total, three relaxation processes are observed in dielectric spectra experimentally. The least-frequency relaxation process P0 is assigned to the dynamics of ions and to the accumulation of charge on the alignment layers. The mid-frequency P1 is the collective orientation of the molecular dipoles around the short axis(flip-flop mode), strongly coupled with the splay fluctuations [8, 11,19,30] in the paraelectric nematic phases. It demonstrates a soft mode like behavior on approaching the ferronematic phase. The high-frequency P2 originates from the polar/chiral domains due to the spontaneous symmetry breaking in achiral mesogen. Both the collective processes, P1 and P2 contribute to the formation of the ferronematic phase. We conclude that there are two independent physical mechanisms for the formation of ferronematic phase, the mechanism in DIO is different than in RM734 compound.

AKNOWLEDGEMENT

One of the authors (NY) thanks the Irish Research Council for awarding the Government of Ireland PDF 2021, GOIPD/2021/858; WJ thanks the CSC, China for award of PhD scholarship.

REFERENCES

[1] T. Niori, T. Sekine, J. Watanabe, T. Furukawa and H. Takezoe, Mater.Chem., **6**, 1231 (1996).

[2] V. P. Panov, M. Nagaraj, J. K. Vij, Yu. P. Panarin, A. Kohlmeier, M. G. Tamba, R. A. Lewis, and G. H. Mehl, Phys. Rev. Lett.,**105**,167801 (2010).

[3] P. Debye, Einige Resultate einer kinetischen Theorie der Isolatoren, Phys. Z, **13**, 97 (1912).

[4] M. Born, Über anisotrope Flüssigkeiten. Versuch einer Theorie der flüssigen Kristalle und des elektrischen Kerr-Effekts in Flüssigkeiten, Sitzungsber. Preuss. Akad Wiss., **30**, 614 (1916).

[5] H. Nishikawa, K. Shiroshita, H. Higuchi, Y. Okumura, Y. Haseba, S. Yamamoto, K. Sago and H. Kikuchi, A fluid liquid-crystal material with highly polar order, Adv. Mater., **29**, 1702354 (2017).

[6] R. J. Mandle, S. J. Cowling and J. W. Goodby, Rational design of rod-like liquid crystals exhibiting two nematic phases, Chemistry-a European Journal, **23**, 14554 (2017).

[7] X. Chen, V. Martinez, E. Korblova, G. Freychet, M. Zhernenkov, M. A. Glaser, C. Wang, C. Zhu, L. Radzihovsky, J. E. Maclennan, D. M. Walba and N. A. Clark, Antiferroelectric Smectic Ordering as a Prelude to the Ferroelectric Nematic: Introducing the Smectic Z_A Phase, arXiv:2112.14222 [cond-mat.soft] (2021).

[8] N. Sebastián, M. Copic and A. Mertelj, *Phys. Rev. E,* **106**, 021001 (2022)

[9] R. Mandle, S. Cowling and J. W. Goodby, A nematic to nematic transformation exhibited by a rod-like liquid crystal, Phys. Chem. Phys. Chem., **19**, 11429 (2017).

[10] A. Mertelj, L. Cmok, N. Sebastián, R.J. Mandle, R.R. Parker, A.C. Whitwood, J. W. Goodby and M. Čopič, Splay Nematic Phase, Phys. Rev. X, **8**, 041025 (2018).

[11] N. Sebastián, L. Cmok, R. J. Mandle, M. Rosario de la Fuente, I. Drevenšek Olenik, M. Čopič and A. Mertel, Ferroelectric-ferroelastic phase transition in a nematic liquid crystal, Phys. Rev. Lett., **124**, 037801 (2020).
[12] R. J. Mandle, S. J. Cowling and J. W. Goodby, Structural variants of RM734 in the design of splay nematic materials, Liq. Cryst., **48**, 1780 (2021).
[13] R. J. Mandle, N. Sebastián, J, Martinez-Perdiguero and A. Mertelj, On the molecular origins of the ferroelectric splay nematic phase, Nat. Comms., **12**, 4962 (2021).
[14] X. Chen, E. Korblova, D. Dong, X. Wei, R. Shao, L. Radzihovsky, M.A. Glaser, J.E. Maclennan, D. Bedrov, D.M. Walba and N.A. Clark, First-principles experimental demonstration of ferroelectricity in a thermotropic nematic liquid crystal: Polar domains and striking electrooptics, Proc. Natl. Acad. Sci. U.S.A., **117**, 14021–14031 (2020).
[15] X. H. Zhao, J. C. Zhou, J. X. Li, J. Kougo, Z. Wan, M. J. Huang and S. Aya, Spontaneous helielectric nematic liquid crystals: Electric analog to helimagnets, Proc. Natl. Acad. Sci. U.S.A., **118**, e2111101118 (2021).
[16] A. Manabe, M. Bremer and M. Kraska, Ferroelectric nematic phase at and below room temperature, Liq Cryst., **48**, 1079 (2021).
[17] R. Saha, P. Nepal, C. Feng, M. S. Hossein, M. Fukuto, R. Li, J. T. Gleeson, S. Sprunt, R. J. Twieg and A. Jákli, Multiple ferroelectric nematic phases of a highly polar liquid crystal Compound, Liq. Cryst. Doi: 10.1080/02678292.2022.2069297 (2022).
[18] D. Pociecha, R. Walker, E. Cruickshank, J. Szydlowska, P. Rybak, A. Makal, J. Matraszek, J.M. Wolska, J.M.D. Storey, C.T. Imrie and E. Gorecka, Intrinsically chiral ferronematic liquid crystals, arXiv:2112.11887 [Cond-mat.soft] (2021).
[19] S. Brown, E. Cruickshank, J.M.D. Storey, C.T. Imrie, D. Pociecha, M. Majewska, A. Makal, and E. Gorecka, Multiple polar and non-polar nematic phases, Chem. Phys. Chem., **22**, 2506 (2021).
[20] Yu. P. Panarin, H. Xu, S. T. Mac Lughadha, and J. K. Vij, Dielectric Response of Ferroelectric Liquid Crystal Cells, Jpn. J. Appl. Phys., **33**, 2648 (1994).
[21] H. Xu, Yu. P. Panarin, J. K. Vij, A. J. Seed, M. Hird and J. W. Goodby, Investigation of the TGBA* phase in a ferroelectric liquid crystal using dielectric spectroscopy, J. Phys.: Condens. Mater., **7**, 7443 (1995).
[22] Yu. Panarin, H. Xu, S. T. Mac Lughadha, J. K. Vij, A. J. Seed, M. Hird and J. W. Goodby, An investigation of the field-induced ferrielectric subphases in antiferroelectric liquid crystals, J. Phys.: Condens.Mater., **7**, L351 (1995).
[23] Yu. P. Panarin, O. E. Kalinovskaya, J. K. Vij and J. W. Goodby, Observation and investigation of the ferrielectric subphase with high q_T parameter, Phys. Rev. E, **55**, 4345 (1997).
[24] Yu. P. Panarin, O. E. Kalinovskaya and J. K. Vij, The investigation of the relaxation processes in antiferroelectric liquid crystals by broad band dielectric and electro-optic spectroscopy, Liq. Cryst., **25**, 241 (1998).
[25] N. Yadav, V. P. Panov, V. Swaminathan, S. P. Sreenilayam, J. K. Vij, T. S. Perova, R. Dhar, A. Panov, D. Rodriguez-Lojo and P. J. Stevenson, Chiral smectic-A and smectic-C phases with de Vries characteristics, Phys. Rev. E., **95**, 062704 (2017).
[26] S. Sreenilayam, Yu. P. Panarin and J. K. Vij, Dielectric study of liquid crystals with large electroclinic effect, Mol. Cryst. Liq. Cryst., **610**, 63 (2015).
[27] N. Yadav and R. Dhar, Impedance Spectroscopy in Modern techniques of spectroscopy: basics, instrumentation and applications, editor by Dheeraj K. Singh, Manik Pradhan (Springer, 2021), pp. 515-540.

[28] S. Sreenilayam, Yu. P. Panarin, J. K. Vij, A. Lehmann, M. Poppe and C. Tschierske, Development of ferroelectricity in the smectic phases of 4-cyanoresorcinol derived achiral bent-core liquid crystals with long terminal alkyl chains, Phys. Rev. Materials, **1**, 035604 (2017).

[29] N.A. Clark, Xi Chen, J.E. Maclennan, M.A. Glaser, Dielectric spectroscopy of ferroelectric nematic liquid crystals: Measuring the capacitance of insulating interfacial layers. arXiv:2208.09784 (2022).

[30] Nataša Vaupotič, Damian Pociecha, Paulina Rybak, Joanna Matraszek, Mojca Čepič, Joanna M. Wolska and Ewa Gorecka, Dielectric response of a ferroelectric nematic liquid crystalline phase in thin cell. arXiv:2210.04697v1 (2022).

[31] Yadav, N., Panarin, Y. P., Jiang, W., Mehl, G. H., & Vij, J. K. (2022). Spontaneous Symmetry Breaking and Linear Electrooptic Response in the Achiral Ferronematic Compound. Technological University Dublin. DOI: 10.21427/MV4X-YK73 https://arrow.tudublin.ie/engscheleart2/317/ **.**

[32] C. Dressel, T. Reppe, M. Prehm, M. Brautzsch, and C. Tschierske, Chiral self-sorting and amplification in isotropic liquids of achiral molecules. Nature Chem. **6**, 971 (2014).

[33] H. Nishikawa and F. Araoka. A New Class of Chiral Nematic Phase with Helical Polar Order. *Adv. Mater*. **2021**, 2101305 (2021).